ELSEVIER

Colloids and Surfaces B: Biointerfaces 20 (2001) 63–72

COLLOIDS AND SURFACES B

www.elsevier.nl/locate/colsurfb

Flunitrazepam induces geometrical changes at the lipid–water interface

María A. Perillo *, Daniel A. Garcia

Cátedra de Química Biológica, Facultad de Ciencias Exactas, Físicas y Naturales, Universidad Nacional de Córdoba. Av.Velez Sarsfield 299, 5000 Córdoba, Argentina

Received 14 March 2000; accepted 17 April 2000

Abstract

Flunitrazepam (FNTZ) effects on molecular packing and surface curvature in artificial model membranes were investigated. FNTZ, from the subphase under dipalmitoylphosphatidylcholine (dpPC) monolayers at the air–water interface, expanded the surface pressure-area isotherm and induced an increment in the limiting area; in this conditions, the collapse pressure of dpPC decreased, indicating a lowering in the stability of the monolayer. Thermodynamic–geometric correlations based on molecular parameters predicted a decrement in the aggregation number and stability, and an increase in the curvature of the self-aggregated structure of dpPC in aqueous medium in the presence of FNTZ. Accordingly, negative-staining electron microscopy of dpPC aqueous dispersions showed that the mean diameter of dpPC vesicles decreased 2 and 2.87 times in the presence of 10 nM and 50 μM FNTZ, respectively, compared with control samples. The release of a soluble marker entrapped in dpPC liposomes increased slightly respect to the control in the presence of FNTZ. In dpPC–dpPE mixed liposomes 50 μM FNTZ induced a decrement in the amount of the aminophospholipid exposed to the outer monolayer. Concluding, an FNTZ-induced expansion of dpPC–water interface region affected the constraints imposed on the lipid–water system by the molecular geometry, interacting free energies and entropy that determine the shape of a multimolecular structure. In liposomes composed of a pure phospholipid, the bilayer expansion leaded, through a structure instability, to reduce the liposome size; in mixed liposomes, phospholipid molecules translocation could be observed as another compensating mechanism of the initial perturbation. These results may be relevant for understanding benzodiazepines' effects non-mediated by membrane receptors.

Keywords: Flunitrazepam; Dipalmitoylphosphatidylcholine self-assembly; Monomolecular layers; Multilamellar vesicles; Electron microscopy; [^{3}H]GABA entrapment; Aminophospholipid translocation

Abbreviations: FNTZ, flunitrazepam; dpPC, dipalmitoylphosphatidylcholine; dpPE, dipalmitoyl phosphatidylethanolamine; MLV, multilamellar vesicles, TNBS, tri-nitro-bencene-sulphonic-acid; [^{3}H]-GABA, [^{3}H]-gamma-aminobutyric acid.

* Corresponding author. Fax: + 54-351-4332097.

E-mail address: mperillo@com.uncor.edu (M.A. Perillo).

0927-7765/01/$ - see front matter

PII: S0927-7765(00)00171-5

1. Introduction

Benzodiazepines (BZDs), which are drugs extensively used as anxiolytics, miorelaxants, anticonvulsants and hypnotics [1,2], can also exert other actions like the inhibition of convulsions induced by maximum electric shock [3], inhibition of status epilepticus [4,5], modification of ionic conductances [6,7], antagonization of voltage dependent Ca^{++} channels [8], inhibition of Ca^{++}-calmodulin protein kinase activity [9], regulation of esteroidogenic enzymes [10], induction of teratogenic effects [11] and relaxant effects on contractile responses induced by KCl and acethylcholine in the presence of Ca^{++} [12], etc. However, only the former effects could be correlated to their ability for binding specifically to membrane proteins at thoroughly studied receptors.

BZDs also interact nonspecifically with the lipidic part of the membrane [13–16]. We have shown a significantly lower tendency of 1,4-BZDs for partitioning into a biological membrane (an anisotropic medium) compared with that for partitioning into octanol (an isotropic medium), the solvent frequently used as a membrane model [16]. Therefore, the membrane-buffer partition coefficient values (P) represent an average value of the preference (compared with an aqueous phase) of BZDs to establish nonspecific interactions with molecules present in the different phases within biological membranes [16]. The P value for FNTZ is strongly influenced by the physical state of the bilayer membrane, whose changes may be triggered by external parameters like temperature and composition as well as by the characteristics of the surrounding media like pH and ionic strength. Particular interactions may lead to strong local accumulation of FNTZ within the membrane due to a coupling to lateral density fluctuations [17,18].

Small foreign molecules interacting with the lipid bilayer may behave either as sustitutionally or as interstitially embedded molecule. This is not necessarily related to the drug molecular size but rather to its amphipathic nature and to its specific interaction with the polar-head group region of the lipid bilayer [19]. A lot of evidence indicates that BZDs behave as substitutional impurities:

1. The decrease in the value of P as the proportion of cholesterol in dpPC–cholesterol mixed liposomes increases [18], in spite of the facts that the partition of FNTZ is favored in more fluid interfaces and that cholesterol is known to decrease the order of crystalline lipid phases [20]; this result has been explained by the assumption that possible vacancies which might incorporate FNTZ are already filled with cholesterol thus inhibiting further FNTZ incorporation [18,21],
2. The localization of BZDs at the polar head group region of highly packed membrane structures was demonstrated by: (a) the delay in the elution time of the peak of dpPC in molecular filtration through Sephadex G-200 [17]; (b) by studies on BZDs acid–base equilibrium in heterogeneous systems [22,23]; and (c) by EPR using probes with the spin label at different positions of the hydrocarbon chain [24].

Packing properties of molecules in bilayer and non-bilayer structures of membranes depend on thermodynamic factors coupled to molecular geometry. The restrictions imposed on the interfacial spontaneous curvature derived from the molecular shape is represented in the dimensionless critical packing parameter $P = v/(a_0 l_c)$ where a_0 is the lipid optimal molecular area, v is the hydrocarbon volume, and l_c is the maximum length of hydrocarbon chains [25,26]. A small molecule located in membranes at the polar head group region would be expected to induce an expansion of the molecular area a_0, a decrease in the value of the critical packing parameter and an increase in the curvature of the interface. Such phenomena are relevant for understanding the pharmacological effects of drugs, e.g. structural rearrangements among bilayer and non-bilayer phases participate in many cellular processes mediated by membrane interactions, recombination and signaling [27–30]. In the present paper we investigated the effects of flunitrazepam on molecular packing and surface curvature in artificial model membranes.

2. Materials and methods

2.1. Materials

FNTZ (7-nitro-1,3-dihydro-1-methyl-5-(2-fluorophenyl)-1,4-benzodiazepin-2-one) was from Hoffman La Roche (Basle, Switzerland). Phospholipids were from Avanti Polar Lipids (Alabaster). [^{3}H]-GABA was purchased from New England Nuclear Chemistry (E.I. DuPont de Nemours, Boston, MA) and TNBS from Sigma Chemical (St Louis, MO). Water was bidistilled in an all-glass apparatus. Other drugs and solvents used were of analytical grade.

2.2. Preparation of lipid dispersions

Liposomes were prepared by evaporating, under a reduced pressure, a chloroformic solution of phospholipid; the dry lipid was suspended in 10 mM Tris-HCl, 140 mM NaCl, pH 7.4 by repeating six consecutive cycles of heating at 60°C for 2 min and vortexing for 30 s. The lipid suspension was stored at room temperature and used within 24 h.

2.3. Incubation system

Before being used, the suspension, maintained at 21°C, was diluted at a final lipid concentration of 1.67 mg ml^{-1} with the same buffer. Experiments were performed in triplicate.

2.4. Transmission electron microscopy

These experiments were performed essentially as in Maggio et al. [31]. Liposomes prepared as indicated above, were incubated for 24 h at room temperature in the presence of FNTZ at a final concentration of 0, 10 nM or 50 μM. An aliquot of the incubate was diluted with sodium phosphotungstate (2% w/v) (the osmolarity was kept at 300 mosM with NaCl), mounted on the carbon grids and observed with a Phillips EM 300 electron microscope operating with an objective aperture of 20 mm and accelerating voltage of 60 KV. For determining average sizes of the structures, 200 measurements were done from pictures taken from representative fields of at least two different preparations.

2.5. Entrapment into liposomes and flunitrazepam-induced release of [^{3}H]GABA

Dry dpPC was dispersed in 50 mM, pH 7.4 Tris-HCl buffer containing [^{3}H]GABA (70 μM). Non-trapped [^{3}H]GABA was eliminated by centrifugation (30|000 × *g*, 15 min). The [^{3}H]GABA-filled liposomes obtained, were resuspended in the same buffer, without radioligand, containing or not FNTZ 22 μM and then, they were incubated between 15 min. and 48 h at room temperature. The radioactivity released was measured, in a 50 μl aliquot of the supernatant, by scintillation spectrometry in a Rackbeta LKB 1224 scintillation counter with a precision of 5% and a counting efficiency of 47% for tritium. Control samples (100% release) was determined by the addition of 10 ml of Triton X-100 (5% V/V final concentration) in order to destabilize the liposomes.

2.6. Determination of the amount of dpPE in the external surface of dpPC–dpPE mixed liposomes

Labeling of aminolipids with TNBS was performed essentially as described by Gruber and Schindler [32]. Mixed dpPC-dpPE (95:5 molar ratio) liposomes were prepared as indicated above using 0.2 M borate buffer pH 9, containing 1 M sucrose. The samples were incubated for 2 h at 45 min, in the absence (control) or in the presence of 50 μM FNTZ (final concentration). Trinitrophenylation was started with TNBS at a final concentration of 0.03%V/V. The reaction was stopped after 30 min of incubation in darkness by the addition of 1.5 M HCl. In blank samples, HCl was added before TNBS in order to inhibit the trinitrophenylation reaction. The percentage of the initial dpPE in the external surface of the outer lamella remaining after the treatment with FNTZ was calculated as:

$$\%\text{dpPE} = \frac{\Delta A_{\text{with, FNTZ}} \times 100}{\Delta A_{\text{without, FNTZ}}} \quad (1)$$

where $\Delta A = A_{410} - A_{530}$ implies a correction for light scattering.

2.7. Monomolecular layers at the air–water interface

Monolayers were prepared and monitored as previously described [33]. The equipment used was a Monofilmmeter (Mayer Feintechnik, Göttingen, Germany) with a circular (Fromherz-type) Teflon-coated trough, having several compartments of different surface area and volume. The equipment is fitted with two barriers that can move independently or synchronously by electronic switching. The signal corresponding to the surface area (automatically determined by the Monofilmmeter according to the relative position of the two compression barriers) and the output from the surface pressure transducer (measured automatically by the Monofilmmeter with a platinized Pt foil 12.5 mm wide × 20 mm long × 0.025 mm thick) were fed into a double-channel $X–Y–Y$ recorder (Yokogawa Corporation, Japan). Before each experiment, the trough was rinsed and wiped clean with 70% ethanol and several times with bidistilled water. The molecular areas of dpPC at different surface pressures were measured in a compartment with an initial surface area of 80 cm^2. The absence of surface-active compounds in the pure solvents and in the subphase solution (buffer 10 mM Tris-HCl, 140 mM NaCl, pH 7.4 with or without FNTZ 10 μM) was checked before each running by reducing the available surface area to less than 10% of its original value after sufficient time was allowed for adsorption of possible impurities that might be present in trace amounts in the subphase. Lipid monolayers were spread by depositing a volume between 10 and 20 μl onto the aqueous surface from solutions in chloroform–methanol 2:1. After 5 min, the monolayer was compressed at a constant rate of 3.6 $cm^2\ min^{-1}$ at 27 ± 1°C. Reproducibility was within ± 0.03 nm^2 and ± 1 mN m^{-1} for molecular and surface pressure, respectively.

2.8. Theoretical calculations

The compressibility modulus [34] was calculated from the virial expansion of the monolayer surface pressure as:

$$K_{A,m} = k \cdot T[1/a] + 2B_2/a^2 + 3B_3/a^3 + \ldots \quad (2)$$

where k is the constant of Boltzmann (1.38×10^{-23} J °K^{-1}) and T is the absolute temperature in °K.

The cohesive intermolecular interaction energies (London–Van der Waals) was calculated according to Salem [35] as in Eq. (3), considering the 16 methylene pairs in the hydrocarbon chain of dpPC:

$$E = \frac{3 \cdot a \cdot \pi \cdot n}{8 \cdot l \cdot d^5} \quad (3)$$

where a, 5600 KJ mol^{-1}; n, number of pairs of methylene groups; l, bond length between methylene groups (0.1253 nm); and d, distance between hydrocarbon chains (half the diameter calculated from molecular area)

The thermodynamic–geometric correlations were based on the Israelachvili's theory for explaining self-assembly of amphiphiles in aqueous medium. The critical packing parameter ($P_c = v/a_o l_c$) allowed the prediction of possible structures compatible with the molecular parameters determined in monolayers. Values of $0 < P_c < 0.5$ corresponded to micelles of different shapes, values of P_c between 0.5 and 1.00 would correspond to bilayer vesicles, and above 1.00, although not predicted by the theory, might indicate the possible formation of hexagonal II phases [25,36].

The minimum free energy per molecule in the aggregate structure is $\mu_o^N = 2\gamma a_o$, where γ is the interfacial free energy and a_o is the optimal molecular area. The aggregation number N is always the smallest one compatible with the lowest value of μ_o^N allowed by a_o.

2.9. Statistical calculations

The propagation error method was applied in every case where the S.E.M. corresponded to a quantity that was calculated from several other measured variables [37]. A two-tailed Student's t-test was used for comparisons [38].

3. Results

Fig. 1a shows the pressure–area (π–A) isotherms of dpPC on 10 mM Tris-HCl, 140 mM NaCl with or without 10 μM FNTZ. At the present assay temperature (27°C), the typical liquid expanded to liquid condensed two-dimensional phase transition characteristic of dpPC isotherm at 21°C although evident, is not very extended along the X axis. In the presence of FNTZ in the subphase, the whole isotherm is displaced to the right and becomes highly expanded at low pressures if compared with the isotherm obtained in the absence of the drug. The limiting area increases from 0.42 nm^2 in the absence of FNTZ to 0.714 nm^2 in its presence and the collapse pressure decreases from 54 to 49 mN m^{-1} (Fig. 1, Table 1).

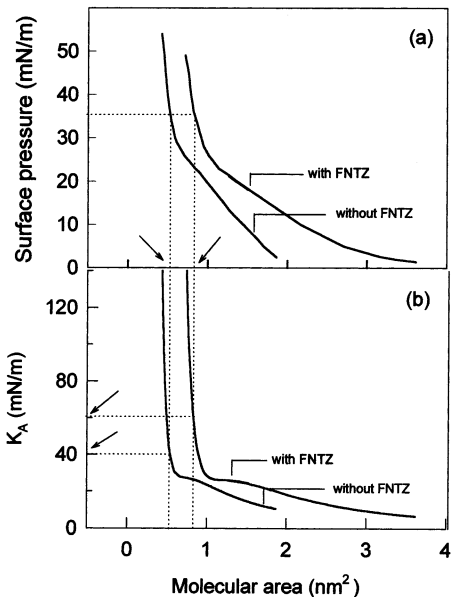

Fig. 1. Effect of flunitrazepam on pressure–area compression isotherms of monomolecular films of dipalmitoylphosphatidylcholine at the air–water interface. (a) Monomolecular films of dpPC were prepared on subphases of 10 mM Tris-HCl/140 mM NaCl pH 7.4 buffer with or without 10 μM FNTZ at 27°C. Experimental details indicated in Section 2. (b) Compressibility modulus K_A as a function of molecular area was calculated by Eq. (2). The values of K_A corresponding to the molecular area at 35 mN m^{-1} (arrows in panel a) both in the presence and absence of FNTZ are indicated by the arrows in panel b.

Table 1
Effect of FNTZ on the molecular and self-aggregation parameters of dpPC[a]

Parameter (units)	Without FNTZ	With FNTZ
1. Limiting area (nm^2)	0.42	0.714
2. Collapse pressure (mN m^{-1})	54	49
3. Molecular area (nm^2)	0.525	0.819
4. E (KJ mol^{-1})	−73.87	−24.30
5. Compressibility modulus (mN m^{-1})	40	61
6. P_c	0.8022	0.5142
7. R_0 (nm)	7.2	2.9
8. R_{out}/R_{in}	1.52	2.68
9. Bilayer thickness (nm)	3.488	2.236
10. μ_o^N (KJ mol^{-1})	1.25	1.92
11. N (molecules/vesicle)	3637.5	253.7

[a] Parameters 1–3 were taken from the surface pressure–area isotherms of Fig. 1. Limiting area is taken at the collapse pressure point (π_c).Values 3–11 were calculated with a value of molecular area taken at 35 mN m^{-1}. Value 5 was determined from Eq. (2) using virial coefficients coming from the adjustment of the π–A isotherms to a virial expansion state equation. Values 6–11 were calculated according to Israelachvili [25,36] using the program Autagrid [39].

The π–A isotherms could be adjusted, particularly in the condensed region, to the virial expansion of the state equation and the following virial coefficients could be determined: $B_2 = 3.43 \pm 2.05$ nm^2, $B_3 = 1.79 \pm 3.9$ nm^4, $B_4 = -2.82 \pm 2.4$ nm^6, $B_5 = 0.76 \pm 0.46$ nm^8 in the absence of FNTZ and $B_2 = 3.64 \pm 0.27$ nm^2, $B_3 = 23.84 \pm 2.28$ nm^4, $B_4 = -36.3 \pm 4$ nm^6, $B_5 = 14.45 \pm 1.7$ nm^8, in the presence of FNTZ. These values of the virial coefficients fed into Eq. (2) let us determine the isothermal elastic modulus of area compressibility (K_A).The value of K_A increased at high π (low areas) and also due to the presence of FNTZ at constant molecular area (Fig. 1b).

Table 1 summarizes the effect of FNTZ on molecular parameters obtained from surface pressure–area isotherms in monolayers at the air–water interface, both at collapse pressure and at 35 mN m^{-1}. The last value was chosen because it is within the a range of possible values for bilayer's internal pressure [34].

Cohesive intermolecular interaction energies (E), calculated according to Eq. (3) and molecular parameters for the self-aggregation of dpPC in the presence and absence of FNTZ calculated according to the self-assembly theory of Israelachvili [33,36,39] are also shown in Table 1. In the presence of FNTZ, we determined a less negative value for the cohesive intermolecular interaction energy indicating a decrease in the stability of the assembly. The value of P_c in the absence of FNTZ (0.8022) predicted the tendency of dpPC for self-aggregating into bilayer vesicles while in the presence of the drug, P_c decreased markedly to 0.5142, a value still above the limit for vesicle forming although quite close to the micellar forming range (the formation of micelles is predicted when the value of P_c is between 0 and 0.5). This result is consistent with the increase in the curvature of the surface (decrement in the theoretical vesicle radius from 7.2 nm in the absence of FNTZ to 2.9 nm in its presence; only qualitative significance should be given to the values predicted for vesicle radius. In addition to the decrease in the vesicle mean size, the theory also predicted a 14.33-fold decrease in the aggregation number as well as a decrease in the stability of the structure (μ_0^N increased from 1.25 to 1.92 KJl mol^{-1}) in the presence of FNTZ compared with the values obtained in its absence.

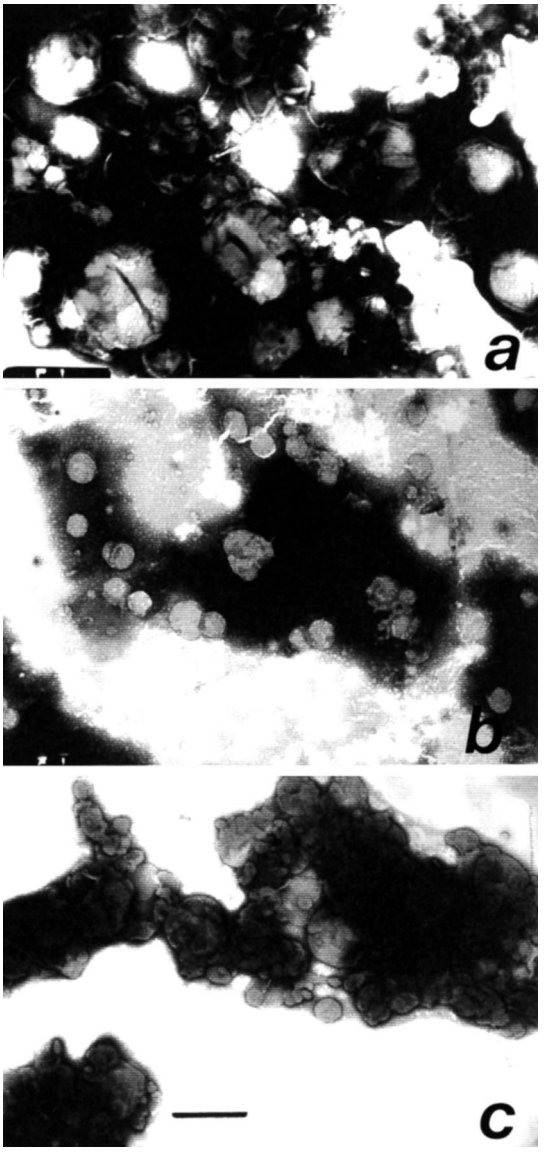

Fig. 2. Effect of flunitrazepam on the size of dpPC liposomes. Electron micrographs of negative stained dpPC aqueous dispersions in the absence (a) or in the presence of FNTZ at a final concentration of 10 nM (b) or 50 μM (c). Pictures were taken from the most representative fields of each sample. Magnification was 12 000 ×. Bar corresponds to 1 μm.

The electron micrographs of negative stained dpPC aqueous dispersions from Fig. 2 showed an effect of FNTZ on reducing the size of dpPC liposomes; FNTZ concentrations used were: 0 (Fig. 2a), 10 nM FNTZ (Fig. 2b) or 50 μM (Fig. 2c). The size distribution of dpPC–liposomes in samples like those shown in Fig. 3 was analyzed as indicated in Section 2. Weighted means $(D) \pm$ S.E.M. are shown in Fig. 3. An important displacement of the distribution curves to lower diameter values was observed as a function of FNTZ concentration. Mean liposome diameter decreased from 525 ± 33 nm in the absence of FNTZ to 255 ± 20 in the presence of 10 nM FNTZ and 183 ± 10 nm in the presence of 50 μM FNTZ. A magnified view of a liposome in the presence of FNTZ (Fig. 4) suggested that the reduction in liposomes mean size occurred through the formation of small vesicles from the outer lamellas of bigger multilamellar liposomes. In order to investigate this hypothesis, we performed an experiment to measure the effect of FNTZ on liposome stability. The percentage of [^{3}H]GABA entrapped inside dpPC liposomes,

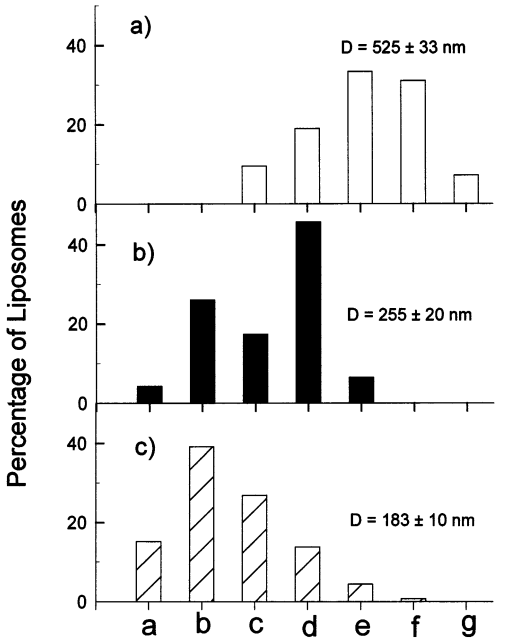

Fig. 3. Size distribution of dpPC–liposomes. Data were taken from the analysis of electron micrographs like those shown in Fig. 2. Between 48 and 200 liposomes were measured in each field. Weighted means (D) ± S.E.M are shown. Panel a: without FNTZ; panel b: 10 nM FNTZ; panel c: 50 μM FNTZ. Letters in abscissa correspond to the following size rages: a = 0–85 nm; b = 86–165 nm; c = 166–250 nm; d = 251–415 nm; e = 416–585 nm; f = 586–835 nm; g = 835 + nm.

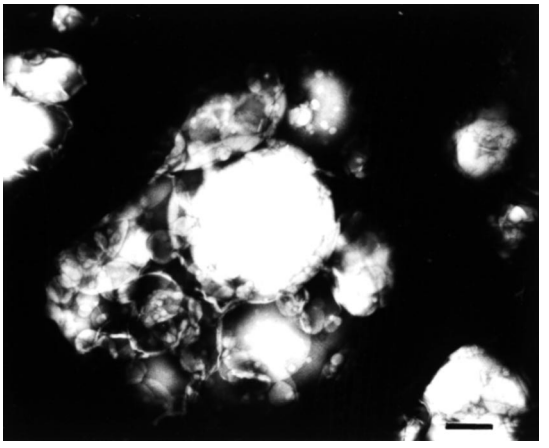

Fig. 4. Effect of flunitrazepam on the destabilization of dpPC liposomes. Electron micrograph of negative stained dpPC aqueous dispersions in the presence of 50 μM FNTZ. A big liposome surrounded by many small vesicles is shown. Magnification was 30 000 ×. Bar corresponds to 0.25 μm.

which was released as a function of time in the presence of FNTZ was not statistically different from that in the absence of the drug up to 24 h of incubation; after 48 h of incubation, the percentage of hydrophilic radioligand released increased significantly in the presence of FNTZ compared with its absence (Table 2).

FNTZ induced a decrement of the amount of dpPE in the external surface of dpPC–dpPE mixed liposomes (Table 3).

4. Discussion

In the study of the effects of drugs on biological membranes, an important question comes up as to which concentration regime of the foreign molecules is the relevant one [40,41]. It has been pointed out that so-called clinical concentrations only have little meaning. From the point of view of physiological effects, the interesting quantity may not necessarily be the global concentration, since thermodynamic lateral heterogeneity of the cooperative membrane assembly may lead to regions with local concentrations that may be higher than the global ones [19]. The lipid phase state may affect the capacity of BZDs for partitioning into the membrane [17,18] and so, modulate its ability to exert their pharmacological effects. Conversely, BZD-membrane interactions involving lipidic domains may alter the delicate dynamics of lipid organization through changes in their phase state [24,42,43] as well as in the intermolecular packing (present paper). As shown in Fig. 1 FNTZ could be incorporated to the interface from the subphase inducing a significant expansion of the monomolecular layer accompanied by a decrease in monolayer stability, as indicated by the lower values of collapse pressure observed in the presence of FNTZ compared with those in its absence (Fig. 1, Table 1).

In the absence of external stress, lipid bilayers are in a tension-free state because at equilibrium the internal pressure in the bilayer, which corresponds to the non-vanishing surface pressure in monolayers, is balanced by the cohesive hydrophobic interaction that is responsible for the bilayer assembly. Therefore, the lateral pressure

within lipid bilayers manifest itself directly in the lateral compressibility only when the membrane is subject to a lateral stress [34]. An elastic compression can arise with the insertion of a foreign molecule in the membrane and will create a non-zero tension T, with a magnitude depending on the K_A, on the molar fraction of drug in the membrane and on the increase in area upon drug insertion. Following this rationale it is clear that the higher the compressibility modulus, the higher would be the tension generated upon drug incorporation and, as a consequence, lower amounts of drug would be found in the membrane; our previous results from bilayers [18] are in accordance with this conclusions. The results shown in Fig. 1 suggest that FNTZ is present in the monolayer all through the range of π where stable dpPC monolayer can be found. However, it cannot be excluded the possibility that some or most of the molecules adsorbed at low π could be squeezed from the monolayer as π increases. Moreover, even at 35 mN m^{-1} the monolayer might not be saturated with FNTZ as suggested by the value of $K_A = 61$ mN m^{-1} obtained in the presence of FNTZ at 35 mN m^{-1} which is even lower than the highest K_A (at π_c) in the absence of drug, suggesting that the monolayer still admits drug incorporation (note that the limiting area with FNTZ is bigger than that without FNTZ).

Table 2
Release of [^{3}H]GABA entrapped inside dipalmitoylphosphatidylcholine liposomes[a]

Time (h)	Percentage of [^{3}H]GABA released	
	Without FNTZ	With FNTZ
0.25	48.60 ± 2.70	41.65 ± 4.45
3	48.15 ± 3.75	44.25 ± 3.35
24	68.40 ± 1.90	59.30 ± 7.30
48	73.30 ± 6.80	105.10 ± 20.1[b]

[a] Experimental details are explained in Section 2. Values are the mean ± S.E.M. of triplicate determinations.
[b] Significantly different from the control without FNTZ ($P < 0.05$, Student's t-test).

Table 3
Effect of FNTZ on the proportion of dpPE in the outer monolayer of dpPC–dpPE mixed MLVs[a,b]

Sample	[FNTZ] (μM)	% dpPE with respect to control
Control	0	100
Experimental	50	43

[a] MLVs, multilamellar vesicles of dpPC:dpPE (95:5 molar ratio).
[b] Values shown are mean ± S.E.M. of triplicates.

As relative small modifications in molecular packing can be amplified into marked changes of the lateral surface pressure, local intermolecular interactions, as well as into long-range alterations of the membrane curvature and phase state [33,44], the recognition and interaction of the membrane with enzymes, toxins, immunological agents, and with other membrane surfaces can be affected as well [45,46]. We showed a dramatic decrement in the diameter of dpPC vesicles induced by the presence of FNTZ (Figs. 2 and 3) at concentrations in the bulk aqueous phase which can be considered as pharmacologically relevant [13]. These result could be predicted by applying Israelachvili's self-assembly theory to the values of molecular areas obtained from monolayer experiments (Table 1) and was consistent with previous studies from our laboratory [14], which let us demonstrate that membrane-BZDs nonspecific interactions could be explained by a partition equilibrium model (unlimited incorporation of molecules). The thermodynamic result of the partition equilibrium is consistent with drug molecules accommodated between lipid molecules, becoming an integral part of the bilayer and inducing its swelling until it converts into a non-bilayer phase [47]. The present studies confirm this fact, at least in the case of FNTZ–dpPC vesicles interaction.

The method used for preparing dpPC liposomes explained in Section 2 was considered as capable of leading to the formation of multilamellar vesicles [48]. The multilamellar condition of the liposomes in our electron micrographs from Figs. 2 and 4 might be questioned however, it was described that multilamellas might not always be evident by negative staining electron microscopy [49]. We interpreted the image from Fig. 4 as a big liposome surrounded by small vesicles formed, probably, at expense of outer lamellas becoming

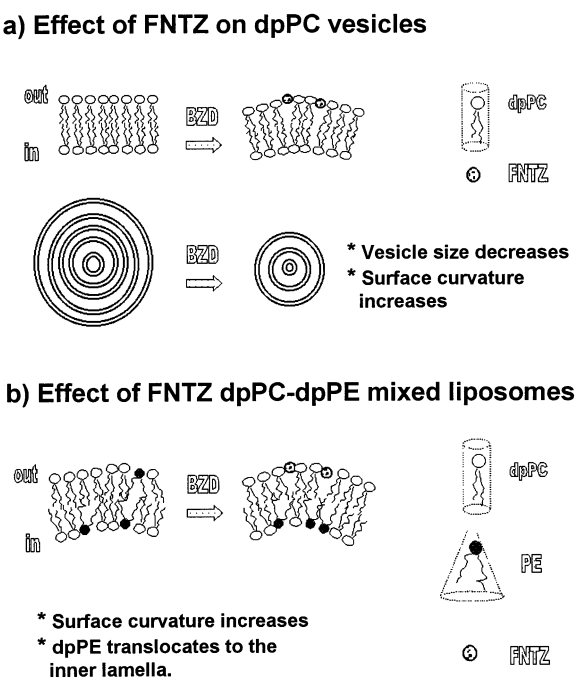

Fig. 5. Model of FNTZ–membrane interaction. DpPC may be represented by a cylindrical molecule (critical parameter value between 0.5 and 1) and dpPE as a truncated cone ($P_c > 1$). FNTZ might be capable of partitioning between both monolayers although, is more concentrated in the outer one. (a) The incorporation of FNTZ in pure dpPC MLVs induce a decrease in the size of the vesicle; and (b) in mixed liposomes in the presence of FNTZ, a flux of the aminophospholipid from the outer to the inner membrane leaflet occurs as another responsive mechanism.

from the bigger one. This interpretation was supported by our results from the release of [^{3}H]GABA entrapped in liposomes. [^{3}H]GABA, as a hydrophilic substance, is expected to be located within polar regions of the liposome, e.g. the water in the core of the liposome or the region within the lamellas. Taking into account the relationship between the volumes of both compartments, it could be stated that the bulk of [^{3}H]GABA entrapped should be in the core of the liposome. The small differences in [^{3}H]GABA released in the presence of FNTZ compared to what happened in its absence was compatible with the rupture of the smaller compartment with a reduction of lamellarity as a consequence of the destabilizing effect exerted by FNTZ.

The decrement in the amount of dpPE in the outer monolayer induced by FNTZ in mixed MLVs, agreed with theoretical predictions of amphiphiles self-assembly based on geometric–thermodynamic concepts mentioned above [36]. Also, experimental data [49] indicated that dpPE, due to geometrical restrictions (presence of a relatively small polar group compared with the volume of hydrocarbon chains), tended to locate preferentially in the inner monolayer, as the bilayer curvature radius decreased. At a pH higher than its pK in water, FNTZ is a neutral molecule that may be able to contact both lamellas of a bilayer. However, as the molecular packing of the external monolayer is lower than that of the inner monolayer and taking into account the tendency of FNTZ to increase its partitioning in low-order interfaces [18] it is expected that FNTZ could be more concentrated in the outer monolayer. Compensating fluxes of dpPE assumed to be of a passive nature might have been generated by the mechanical stress originated by FNTZ-induced membrane curvature increase. Similar phenomena may be triggered by the activity of flippase and aminophospholipid translocases in natural membranes [50].

Concluding, the present results indicated that FNTZ, by interacting with the dpPC–water interface, reduced the molecular packing; this fact leaded to an increase of the relative volume of the polar head groups region and to a decrease in the thermodynamic stability of the self-aggregating structure which was forced towards an increase in its surface curvature. In membranes of more complex composition, which had more responsive mechanisms, the tensions originated by drug incorporation and curvature increment, could be compensated by fluxed of lipid molecules between outer and inner membrane leaflets changing their lipidic compositions in order to satisfy their spontaneous curvature (Fig. 5). Such phenomenon might trigger some of the pharmacological effects attributed to BZDs.

Acknowledgements

We are grateful to Professor B. Maggio for the use of the Monofilmmeter and the program 'Autagrid' which he wrote for self-assembly parameters calculations. This paper was partly supported by grants from CONICOR, SECYT-Univ. Nac. de Córdoba, FONCYT and CONICET, República Argentina. María A. Perillo is a career investigator and Daniel A. Garcia holds a postdoctoral fellowship from the latter institution.

References

[1] F.A. Stephenson, Biochem. J. 249 (1988) 21.
[2] M. Gavish, Y. Katz, S. BarAmi, R. Weizman, J. Neurochem. 58 (1992) 1589.
[3] H. Möhler, T. Okada, Science 198 (1977) 849.
[4] A.V. Delgado-Escueta, C. Wastertain, D.M. Treimen, R.J. Porter, New Eng. J. Med. 306 (1982) 1337.
[5] W. Ling, D.R. Wesson, in: D.E. Smith, D.R. Wesson (Eds.), The Benzodiazepines, Current Standards for Medical Practice, MTP Press, Hinghan, MA, 1985, p. 149.
[6] J.A. Ferrendelli, S. Daniels-McQueen, J. Pharmacol. Exp. Ther. 229 (1982) 29.
[7] R. Olsen, J. Yang, R. King, A. Dilber, G. Stauber, R. Ranson, Life Sci. 39 (1986) 1969.
[8] W.C. Taft, R.J. DeLorenzo, Proc. Natl. Acad. Sci. USA 81 (1984) 3118.
[9] R.J. DeLorenzo, S. Burdette, J. Holderness, Science 213 (1981) 157.
[10] I. Thomson, R. Fraser, C.J. Kenyon, J. Steroid Biochem. Mol. Biol. 53 (1995) 75.
[11] V.E. Grimm, in: J. Yanai (Ed.), Neurobiological Teratology, Elsevier, Amsterdam, 1984, p. 153.
[12] C. Pérez-Guerrero, M.D. Herrera, E. Marhuenda, J. Pharm. Pharmacol. 48 (1996) 1169.
[13] R.M. Arendt, D.J. Greenblatt, D.C. Liebisch, M.D. Luu, S.M. Paul, Psychopharmacology 93 (1987) 72.
[14] M.A. Perillo, A. Arce, J. Neurosci. Methods 31 (1991) 203–208.
[15] M.A. Perillo, D.A. García, Biomed. Chromatogr. 6 (1992) 183.
[16] M.A. Perillo, D.A. García, A. Arce, Mol. Membr. Biol. 11 (1995) 217.
[17] D.A. García, M.A. Perillo, Biomed. Chromatogr. 11 (1997a) 343.
[18] D.A. García, M.A. Perillo, Colloids Surf. (B) 9 (1997b) 49.
[19] K. Jorgensen, J.G. Ipsen, O.G. Mouritsen, D. Bennett, M.J. Zuckermann, Biochim. Biophys. Acta 1062 (1991) 227.
[20] D. Marsh, I.C.P. Smith, Biochim. Biophys. Acta 228 (1973) 133.
[21] M. Luxnat, H.J. Galla, Biochim. Biophys. Acta 856 (1986) 274.
[22] D.A. García, M.A. Perillo, Biochim. Biophys. Acta 1324 (1997c) 76.
[23] D.A. García, M.A. Perillo, Biochim. Biophys. Acta 1418 (1999) 221.
[24] M.A. Perillo, L.V. Nogueira, S. Schreier, Spin label study of FNTZ-membrane interaction. III Ibero–American Congress of Biophysics, Buenos Aires, 1997, Abstract 157.
[25] J.N. Israelachvili, S. Marcelja, R.G. Horn, Q. Rev. Biophys. 13 (1980) 121.
[26] C. Tanford, J. Phys. Chem. 78 (1974) 2469.
[27] M.Y. Santini, P.L. Indovina, A. Cantafora, I. Blotta, Biochim. Biophys. Acta 1023 (1990) 298.
[28] P.R. Cullis, M.J. Hope, M.B. Bally, T.D. Madden, L.D. Mayer, D.B. Fenske, Biochim. Biophys. Acta 1331 (1997) 187.
[29] N. Maulik, V.E. Kagan, V.A. Tyurin, D.K. Das, Am. J. Physiol. 274 (1998) H242.
[30] M. Przybylska, M. Faber, A. Zaborowsky, J. Swietolawsky, M. Bryszewska, Clin. Biochem. 31 (1998) 73.
[31] B. Maggio, J. Albert, R.K. Yu, Biochim. Biophys. Acta 945 (1988) 145.
[32] H.J. Gruber, H. Schindler, Biochim. Biophys. Acta 1189 (1994) 212.
[33] M.A. Perillo, A. Polo, A. Guidotti, A. Costa, B. Maggio, Chem. Phys. Lipids 65 (1993) 225.
[34] D. Marsh, Biochim. Biophys. Acta 1286 (1996) 183.
[35] L. Salem, J. Chem. Phys. 37 (1962) 2100.
[36] J.N. Israelachvili, Intermolecular and Surface Forces, Academic Press, New York, 1989.
[37] J.R. Green, D. Margerison, Statistical Treatment of Experimental Data, Elsevier, New York, 1978.
[38] R. Sokal, J. Rohlf, Introducción a la Bioestadística, Reverté, Barcelona, 1980.
[39] B. Maggio, Biochim. Biophys. Acta 815 (1985) 245.
[40] T. Yoshida, K. Taga, H. Okabayashi, H. Kamaya, T. Ueda, Biochim. Biophys. Acta 1028 (1990) 95.
[41] E. De Paula, S. Schreier, Biochim. Biophys. Acta 1240 (1995) 25.
[42] T. Mennini, A. Ceci, S. Caccia, S. Garattini, P. Masturzo, M. Salmona, FEBS Lett. 173 (1984) 255.
[43] H. Kurishingal, P. Barain, C. Restall, Biochem. Soc. Trans. 20 (1992) 157S.
[44] M.A. Perillo, N.J. Scarsdale, R.K. Yu, B. Maggio, Proc. Natl. Acad. Sci. USA 91 (1994) 10019.
[45] B. Maggio, R.K. Yu, Biochim. Biophys. Acta 1112 (1992) 105.
[46] B. Maggio, J. Lipid Res. 40 (1999) 930.
[47] A. Seelig, P.R. Allegrini, J. Seelig, Biochim. Biophys. Acta 939 (1988) 267.
[48] A.D. Bangham, M.M. Standish, J.C. Watkins, J. Mol. Biol. 13 (1965) 238.
[49] D. Rickwood, B.D. Hames, in: R.R.C. New (Ed.), Liposomes: a Practical Approach, IRL Press, New York, 1990, p. 105.
[50] S. Frickenhaus, A. Herrmann, R. Heinrich, Mol. Membr. Biol. 15 (1998) 213.